Resistive wall stabilization of short-wavelength edge modes in tokamaks

V.D. Pustovitov[1] and V.V. Yanovskiy[2]

[1] National Research Centre "Kurchatov Institute", Moscow, 123182, Russia

[2] Consorzio RFX, Associazione EURATOM-ENEA sulla Fusione, Padova, 35127, Italy

1. Introduction. Resistive wall stabilization of long-wavelength kink-like modes (resistive wall modes, RWMs) resulting in essential improvement in terms of the achievable beta was discovered and systematically studied on the DIII-D tokamak [1, 2]. The modes called RWMs have low m and n (poloidal and toroidal wave numbers). Typically, $m = 2$ or 3 and $n = 1$ [2]. Analytical theory predicts [3–5] and model computations confirm [6] that such modes can be stabilized by fast enough rotation affecting the energy dissipation in the resistive wall through the skin effect. This looks an attractive possibility to explain still mysterious rotational stabilization in DIII-D [1, 2]. The model is based on the first principles (Maxwell equations and Ohm's law) which implies that the phenomenon must be a part of other events whenever a mode interacts with a wall. To prove this, we extend the approach to a wider area.

Here we analyze a possible effect of the rotational stabilization [3–6] on the modes with m and n higher than those of conventional RWMs. Such modes with $m \leq 10$ are often observed in experiments in tokamaks as oscillations with a saturated amplitude, see [7, 8].

2. Formulation of the problem. We consider the cylindrical plasma with nearby resistive wall of radius r_w and thickness d_w. The plasma-wall gap and space behind the wall are treated as vacuum. As in [6], we have to solve the dispersion relation for the external kink modes

$$g_m = \sqrt{\gamma \tau_{sk}} \frac{K_{m-1}(y_i)I_{m-1}(y_e) - I_{m-1}(y_i)K_{m-1}(y_e)}{K_m(y_i)I_{m-1}(y_e) + I_m(y_i)K_{m-1}(y_e)}, \tag{1}$$

where I and K are the modified Bessel functions of the first and the second order, y_i and y_e are values of $y = \sqrt{\gamma \tau_{sk}} \, r / d_w$ on the inner ($r = r_w$) and the outer ($r = r_w + d_w$) sides of the wall,

$$\tau_{sk} \equiv \mu_0 \sigma d_w^2 \tag{2}$$

and σ is the wall conductivity. This is derived for the (m,n) mode of the magnetic perturbation **b** depending on time as $\exp(\gamma t)$ with $\gamma = \gamma_R + in\omega$ (γ_R and ω are, respectively, the growth rate and the rotational frequency of the mode). The stability parameter $g_m = g_R + ig_I$ on the left-hand side is determined by the plasma properties [3–6] through the boundary conditions for **b** at the plasma boundary. For calculations we take $r_w / d_w = 50$ roughly corresponding to parameters of the DIII-D tokamak.

Equation (1) was derived assuming $n/(mA) \ll 1$ and $A^2 |\gamma| \tau_{sk} \gg n^2 d_w^2 / r_w^2$ where $A = R / r_w$ with R the major radius. In this approximation, n enters the final result (1) through $\gamma_R + in\omega$ only, while the m number is present there as a parameter determining the order of the modified Bessel functions. In the limit $s \ll d_w$, where s is the skin depth determined by $1/s = \text{Re}\sqrt{\mu_0 \sigma \gamma}$, Eq. (1) gives us (for more details and alternative derivations see [3–6])

$$\gamma_R = \gamma_R^{ld}(1 - \omega^2 / \omega_{cr}^2),\tag{3}$$

where $n\omega_{cr} = 2\gamma_R^{ld} = 2g_R^2 / \tau_{sk}$. This explicitly describes the rotational stabilization of the fast rotating modes, but does not show a dependence of m hidden in Eq. (1). In [6], the effect was studied and predictions of Eqs. (1) and (3) have been compared for the $m = 2$ mode. Here similar analysis is performed for m up to 10.

3. Computation results. First, we note that the locked modes ($\omega = 0$ or $g_I = 0$) become unstable at $g_R > 0$. Their normalized growth rate $\gamma_N = \gamma_R \tau_{sk}$ calculated by formula (1) is shown by solid curves in Fig. 1 for $m = 2$ and $m = 10$. At given g_R, the mode with higher m have slightly larger growth rate. Nevertheless, at $g_R > 1$, the solid curve for $m = 10$ is quite close to the parabolic dashed curve representing asymptotic dependence (3). The deviation decreases with increasing g_R. It is under 10% at $g_R > 3.49$ for $m = 10$ and at $g_R > 1.88$ for $m = 2$. The straight line in Fig. 1 corresponds to the standard

Fig. 1. Normalized growth rate $\gamma_N = \gamma_R \tau_{sk}$ versus g_R for the $m = 2$ and $m = 10$ locked modes. The solid curves are calculated by Eq. (1), the dashed one by its thick-wall asymptote (3) at $\omega = 0$ and the straight solid line is the standard thin-wall estimate $\gamma_R \tau_{sk} = g_R$.

thin-wall approach which, indeed, stronger underestimates the growth rate at $g_R > 1$ than the thick-wall model. At the point $g_R = 1$ both asymptotes, linear and parabolic, give 32.5% error for $m = 2$ and 41.7% for $m = 10$.
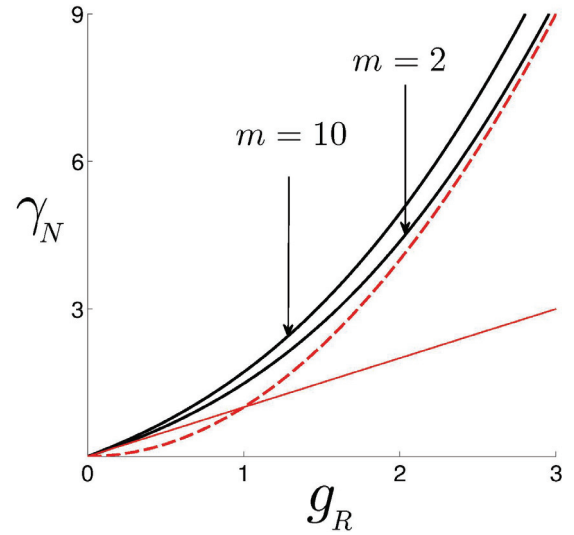
The results in Fig. 2 can be interpreted as a rotation frequency of a marginally stable mode at given g_R. This $\omega_N = \omega \tau_{sk}$ is equivalent to $\omega_N^{cr} = \omega_{cr} \tau_{sk}$, but now it is calculated from Eq. (1) derived without expansions in s/d_w. For comparison, ω_{cr} is plotted here as a dashed

parabolic line. The solid curves represent solutions of Eq. (1) for $m = 2$ and $m = 10$ modes. The modes with higher m numbers give larger ω_N for a given g_R that implies necessity of larger rotation frequencies to stabilize them. The deviation of the solution of Eq. (1) from asymptotic parabola (3) is less than 10% at $g_R > 3.56$ for $m = 10$ and at $g_R > 1.98$ for $m = 2$. At the point $g_R = 1$ the error is 32.7% and 19.5% for $m = 10$ and $m = 2$, respectively.

The rotational stabilization depicted in Figs. 1 and 2 is related to the skin effect in the resistive wall. Solid curves in Fig. 3 show the radial component of the perturbed magnetic field b_r inside the wall for $m = 2$ and $m = 10$ modes at $\gamma_N = 1$ and $\omega_N = 1$. Here the real part of the perturbed magnetic flux $\psi = irb_r / m$ normalized to its value on the inner side of the wall is plotted versus the distance across the wall normalized to its thickness. The horizontal line is the thin-wall asymptote while the dashed curve is the real part of $\exp(-\ell / S)$, where $\ell = (r - r_w) / d_w$ and $1/S \equiv \sqrt{\mu_0 \sigma \gamma}$. Clearly, both solid curves are better approximated
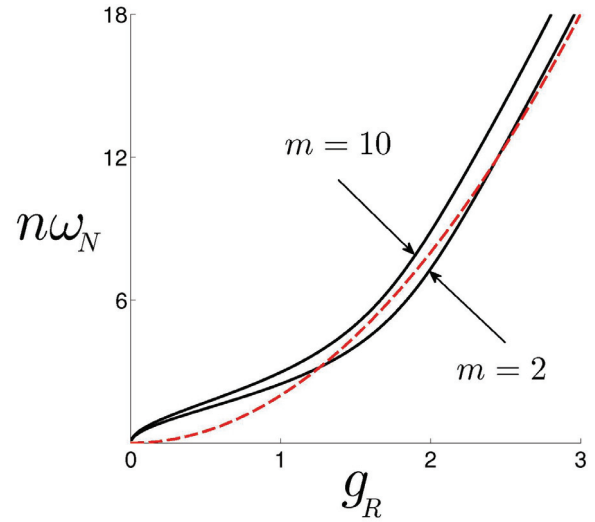

Fig. 2. Minimal angular rotation frequency necessary for the rotational stabilization of the $m = 2$ and $m = 10$ modes at given g_R. The solid curves are calculated by formula (1), the dashed one is the parabola (3).
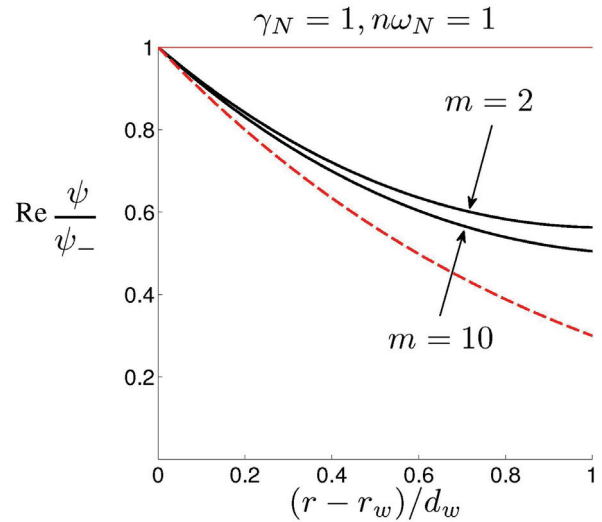

Fig. 3. $\mathrm{Re}(\psi / \psi_-)$ for the $m = 2$ and $m = 10$ modes at $\gamma_N = 1$ and $n\omega_N = 1$ (solid curves). The dashed curve is the real part of $\exp(-\ell / S)$ while the horizontal line corresponds to the thin-wall approach.

by the exponent function than by a constant, which proves that a thin-wall approximation ($\psi = const$ in the wall) cannot be used for these modes. At higher m the mode amplitude stronger decreases with ℓ inside the wall and lies closer to the exponent.

4. Discussion. The presented results show that predictions of (3) derived in the limit $g_R \gg 1$ [3–6] can be used for modes with m from 2 to 10 at $g_R > 1$. In practice this means the

oscillations with frequencies of several kHz, see [9]. The constraint on maximal m comes from the fact that even an ideal wall response must be $(r_p/r_w)^{2m}$ weaker than the driving perturbation at the plasma surface. In our analysis we use $r_p/r_w = 0.9$ to mimic DIII-D [2]. Then for $m = 10$ we have $(r_p/r_w)^{2m} \approx 0.12$ showing a weak, but nonnegligible effect of the wall on the mode. To compare our results with experimental observations, we need τ_{sk}. With $\tau_{sk} = 10^{-4}$ s, which is a good estimate for DIII-D tokamak, the point with $\omega_N = 6.28$ corresponds to the critical frequency $\nu_{cr} \equiv \omega_N/(2\pi\tau_{sk}) = 10$ kHz. Such frequency is typical for EHO's fundamental $m/n = 5/1$ mode in the DIII-D [7]. The ratio r_p/r_w varies strongly among the machines, which can be a reason for discrepancies in observed EHOs in various tokamaks [10, 11].

5. Conclusion. The study proves that the effect of rotational stabilization must play a role in the dynamics of short-wavelength edge modes in tokamaks and hence should be taken into account at their analysis at relatively modest $g_R \sim 1$ or at $n\omega\tau_{sk} \geq 2$. In particular, we expect that the dynamics of EHOs and HFOs [7, 10, 11] can be partly explained by the wall-mode interaction. Moreover, the sensitivity of the results in [8] on the MHD oscillation frequency may also be attributed to the wall effect. For experimental testing of the model predictions the measured growth rates and the frequencies of the edge perturbations should be compared with Eq. (3). It could be helpful to collect the data at different values of the ratio r_p/r_w. The rotational stabilization at $g_R < 1$ (smaller rotation frequencies) is the field of future theoretical studies.

[1] E.J. Strait, *et al.*, Nucl. Fusion **43**, 430 (2003).

[2] M.S. Chu and M. Okabayashi, Plasma Phys. Control. Fusion **52**, 123001 (2010).

[3] V.D. Pustovitov, Phys. Plasmas **19**, 062503 (2012).

[4] V.D. Pustovitov, Nucl. Fusion **53**, 033001 (2013).

[5] V.D. Pustovitov, Plasma Phys. Rep. **39**, 199 (2013).

[6] V.D. Pustovitov and V.V. Yanovskiy, Modelling of the plasma rotational stabilization with account of the skin effect in the resistive wall in tokamaks, to be published in Plasma Phys. Reports **39**, (2013).

[7] N. Oyama, *et al.,* Plasma Phys. Control. Fusion **48,** A171 (2006).

[8] W. Jin *et al.*, Plasma Phys. Control. Fusion **55**, 035010 (2013).

[9] V.D. Pustovitov, Resistive wall effects on the plasma dynamics in tokamaks, P5.148, this Conference.

[10] W. Suttrop, *et al.*, Plasma Phys. Control. Fusion **45,** 1399 (2003).

[11] T.H. Osborne, *et al.,* J. Phys.: Conf. Ser. **123,** 012014 (2008).